Princeton Plasma Physics Laboratory

PPPL-

PPPL-
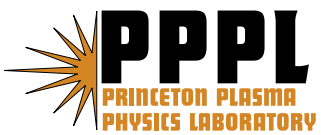
Princeton Plasma Physics Laboratory
Report Disclaimers

PPPL Report Availability

Princeton Plasma Physics Laboratory:

http://www.pppl.gov/techreports.cfm

Office of Scientific and Technical Information (OSTI):

http://www.osti.gov/bridge

Related Links:

U.S. Department of Energy

Office of Scientific and Technical Information

Fusion Links

Electron acceleration in a geomagnetic Field Line Resonance

P.A. Damiano and J.R. Johnson

Princeton Plasma Physics Laboratory, Princeton, New Jersey

_____

_____

A hybrid MHD kinetic electron model in dipolar coordinates is used to simulate the upward current region of a geomagnetic Field Line Resonance (FLR) system for a realistic ambient electron temperatures of a keV. It is found that mirror force effects result in potential drops sufficient to accelerate electrons to energies in excess of a keV in support of field aligned currents on the order of 0.5 μA/m^2. The wave energy dissipated in this acceleration would completely damp an undriven FLR with an equatorial width of 0.5 R$_\text{E}$ within two resonance cycles.

1. Introduction

Field Line Resonances have been linked to the formation of some auroral arcs (e.g. Lotko et al. 1998; Samson et al., 2003) where arcs resulting from electron acceleration within these waves are seen to modulate with the same mHz frequency as the magnetic perturbations associated with the resonance (e.g. Samson et al., 2003). Electrons must be accelerated through a potential drop of a keV in order to power these auroral emissions (e.g. Lotko et al., 1998) which when considering the size of the auroral acceleration region necessitates parallel electric fields on the order of a mV/m. The mechanisms by which sufficient potential drops are generated within global scale waves are not completely understood. Several possibilities have been proposed including, nonlinear electron inertial effects (Wright et al., 2003), the effects of stationary nonlinear inertial Alfvén waves (Knudsen, 1996), anomalous resistivity (Lotko et al., 1998) and mirror force effects (Rankin et al.,1999). All these studies, however, neglect the self-consistent evolution of the electron distribution function with the wave, and so over the last decade, approaches using self-consistent models incorporating electron kinetic effects have been developed. Damiano et al. (2007; 2008) considered the upward current region (corresponding to the downward propagation of magnetospheric electrons) of a toroidal FLR system using a 2D hybrid MHD-kinetic electron model in dipolar coordinates. The significant dissipation of wave energy associated with the acceleration process was illustrated along with the increase in $E_{||}$ evident with increases in the ambient electron temperature up to 200 eV. Rankin et al. (2007) studied a multi-period resonance system using a 1-D uniform plasma model with a Vlasov description for the electrons and illustrated that nonlinear electron

trapping over several periods was a more efficient sink of wave energy than electron Landau damping. In this present study, we extend the work of Damiano et al. (2008) and for the first time consider an FLR system with a realistic electron temperature of a keV (in a proper dipolar geometry) in order to determine the extent of magnetic mirror force effects on $E_{\parallel}$ generation, electron energization and wave dissipation.

The rest of the paper is broken up into four sections. Section 2 summarizes the hybrid model used. Section 3 presents the simulation results while Section 4 gives our conclusions.

2. Hybrid Model

The simulations were performed with a 2-D hybrid MHD-kinetic electron model in dipolar coordinates (Damiano et al., 2007) where the model geometry is illustrated in Figure 1 and explicitly includes the field aligned direction (x_1) and the direction across L shells (x_2). Our system is independent of the azimuthal coordinate so that $\partial/\partial x_3 = 0$. Corresponding to a toroidal FLR, our model combines the linearized cold plasma MHD equations for the azimuthal perturbations of velocity (u_3) and magnetic field (b_3) given respectively by

$$\mu_o \rho_o \frac{\partial u_3}{\partial t} = \frac{B_o}{h_1 h_3} \left(\frac{\partial}{\partial x_1} (h_3 b_3) \right) \tag{1}$$

$$\frac{\partial b_3}{\partial t} = \frac{-1}{h_1 h_2} \left(\frac{\partial}{\partial x_1} (h_2 E_2) - \frac{\partial}{\partial x_2} (h_1 E_1) \right) \tag{2}$$

and the guiding center equations for the electron dynamics

$$m_e \frac{dv_1}{dt} = -eE_1 - \mu_m \frac{1}{h_1} \frac{\partial B_o}{\partial x_1} \qquad (3)$$

$$h_1 \frac{dx_1}{dt} = v_1 \qquad (4)$$

where v_1 is the parallel electron velocity, $x_1 = \cos\theta/r^2$, $x_2 = \sin^2\theta/r$, $x_3 = \phi$, $h_1 = r^3/(1+3\cos^2\theta)^{1/2}$, $h_2 = r^2/(\sin\theta(1+3\cos^2\theta)^{1/2})$, $h_3 = r\sin\theta$ and $\mu_m = m_e v_\perp^2/(2B)$ is the magnetic moment. The solutions of the coupled equations (1) and (2) with $E_2 = -u_3 B_o$ and $E_1 = 0$ will be referred to as the MHD model.

Closure between MHD and electrons is via the parallel electric field which is calculated from a variant of the generalized Ohm's law that incorporates the moments of the electron distribution function along with a closure that enforces quasi-neutrality. For brevity, a detailed discussion of the closure is neglected here, but a complete derivation can be found in Damiano et al. (2007).

Perfectly reflecting boundary conditions are assumed at the ionospheres ($u_3 = j_2 = \partial(h_1 j_1)/\partial x_1 = \partial(h_3 b_3)/\partial x_1 = 0$). At the perpendicular boundaries (along the lines of constant x_2) a node in current is assumed which implies nodes in E_1 and anti-nodes in b_3, j_2 and u_3 (respectively $\partial(h_3 b_3)/\partial x_2 = \partial(h_1 h_3 j_2)/\partial x_2 = \partial/\partial x_2(h_1 h_3 u_3/B_o) = 0$).

Whereas, the fluid equations are solved at the fixed simulation grid points, the electrons are initialized everywhere in the simulation domain such that the density is everywhere constant ($n_e = n_i = 1$ cm^{-3}). A uniform distribution is assumed in velocity space with the exception that the loss cone is empty so that all electrons are initially mirror force trapped within the simulation domain. The choice of starting with an empty loss cone

simplifies the particle boundary conditions, but does not alter the long term evolution of the system (Damiano and Wright, 2008). Electrons accelerated into the loss cone over the course of the simulation precipitate from the simulation domain when they reach the field-aligned simulation boundaries which balances the implied polarization drift of the ions (represented within the cold plasma MHD description) azimuthally out of the computational domain over the course of the simulation. Standard Particle-In-Cell (PIC) techniques are used to interpolate fields to particle positions and construct the moments of the electron distribution function.

The simulations are initialized using the perturbation of the azimuthal velocity illustrated in Figure (2) where the field-aligned profile in panel (b) is the approximate fundamental eigenmode solution along an $L = 10$ magnetic field line (consistent with that used in Damiano and Wright (2008)). The modified half-Gaussian profile in the perpendicular direction (Figure 2a) results in the formation of the upward field aligned current region associated with auroral arc formation. The constant amplitude to the left of the Gaussian tail, centers the resulting current profile (Figure 4) within the simulation domain. The resulting resonance has a period, $T_A = 270$ s.

3. Simulations

Figure 3 displays 2-D image plots of the parallel current density computed from the electrons ($j_1 = j_{||} = j_e$) as a function of x_1 and x_2 in the northern hemisphere of the computational grid for both the MHD and hybrid models at $t = 0.2\,T_A$. In each panel, the left and right hand sides are the equator and northern ionospheric boundary respectively and j_1 rises with the convergence of the magnetic field topology as the ionosphere is

approached. Consistent with the previous studies (Damiano et al., 2007; Damiano and Wright, 2008) the hybrid model displays a coupling of global energy to small perpendicular scale lengths (which fluctuate on the order of seconds) and a broadening of the current profile.

The time evolution of j_1 at the ionospheric boundary is given in the top panels of Figure 4 while the corresponding distribution function evolution in the region of the current maximum (vertical dashed lines in Figure 4a) is displayed in the panels below. The ring distribution evolves from the Maxwellian as accelerated electrons undergo mirroring. In the top panels, j_1 grows with time (along with the ring distribution radius), but eventually broadens and saturates. The saturation is co-incident with the depletion of electrons at small pitch angles and the broadening is a result of the acceleration of electrons along field lines adjacent to the original profile (denoted by the MHD result) where it is easier to accelerate electrons than in the original profile depleted of accessible current carriers. The global characteristics of the broadening and saturation are consistent for both increased grid and particle resolution, but a more detailed analysis of this (and coupling to small perpendicular wavelengths) is beyond the scope of this letter and will be the subject of a subsequent investigation.

The temporal evolution of the energy of the distribution functions illustrated in Figure 4 is plotted in the top panel of Figure 5 where the energy of the accelerated population reaches almost 2 keV by $1/4\ T_A$. In contrast, setting $T_e = 200\ eV$ resulted in a maximum energy of about $800\ eV$ by the same time, illustrating the mirror force effects on the magnitude of the particle energization. An additional interesting feature is the periodic

structuring which is most likely linked to the electron bounce motion (which may also be linked to the fast fluctuations noted previously).

As evident in both observations (e.g. Wygant et al., 2000; Chaston et al. 2002; 2005) and theoretical investigations (e.g. Wright et al., 2003; Lysak and Song, 2003; Damiano et al., 2007) the dissipation of wave energy by electron acceleration can be significant. The magnitude of this dissipation for an FLR system (which is hard to establish from observations alone) can be quantified by summing the ion kinetic and magnetic field energies for both the MHD and hybrid simulations as displayed in the bottom panel of Figure 5. This sum is conserved in the MHD case but in the hybrid case, the ion kinetic energy is being partitioned between the magnetic field and electron energization resulting in the 20% drop relative to the MHD result. An additional 1.5-1.6 times this energy will be transferred into the electron energization by $1/2$ T_A (Damiano et al., 2007) implying that greater than 30% of the initial wave energy would be dissipated by this time. Therefore, an undriven, standing mode would be completely damped in less than two Alfvén cycles (since regions of downward j_1, associated with ionospheric electron acceleration, would likewise draw energy from the wave). In contrast, Damiano et al. (2007) illustrated that a resonance system of similar width, but with $T_e = 5$ eV, dissipated only 5 % of the wave energy by $1/2$ T_A. This dramatic difference is because more energy must be expended to overcome the increased mirror force experienced by a greater number of electrons with increased T_e. Additionally, this dissipation increases nonlinearly with decreased resonance width (Damiano et al., 2007) implying that for realistic T_e, an FLR could be dissipated in under one period.

Figure 6 plots j_1 (at $x_2 = 0.1025$) as a function of potential drop along the field line from the equator to the northern ionospheric boundary where the linear profile results from the choice of a constant density and implies that $\Delta\Phi/B_o$ is constant along the field line at a specific time. As time progresses, the potential drop that the electrons fall through increases up to $1/4$ T_A since the depletion of accessible current carriers requires a progressively larger potential drop to sustain the saturated current density. The value of $E_{||}$, in the auroral acceleration regions, consistent with these potential drops is on the order of several tenths of mV/m.

The $\Delta\Phi$ at a specific time agrees very well with the peak of the electron energization (red band in top panel of Figure 5). This agreement is consistent with the quasistatic nature of the FLR system where energy conservation in the frame of reference of the electrons implies $\Delta\Phi = m_e(v_\perp^2 + v_{||}^2)/2$. Additionally, this agreement illustrates that accelerated electrons are primarily sourced from the distribution bulk, where initial thermal energy is minimized.

4. Conclusions

For the first time, the upward current region of a toroidal FLR system has been studied using a 2-D hybrid MHD kinetic electron model in dipolar coordinates for a realistic ambient electron distribution temperature of a keV. It is found that mirror force effects lead to potential drops large enough to accelerate bulk electrons to observed energies in excess of a keV. The energy dissipated in this acceleration would almost completely damp the resonance within 1-2 periods and thus an FLR system must be strongly driven in order to persist for much longer time scales. Additionally, the field aligned current in the hybrid

MHD-kinetic electron system saturates approximately consistent with the depletion of the availability of electrons at small pitch angles and electrons are accelerated along adjacent field lines in order to carry the field aligned current.

References

Chaston, C.C., J.W. Bonnell, L.M. Peticolas, C.W. Carlson, J.P. McFadden, and R.E. Ergun (2002), Driven Alfvén waves and electron acceleration *Geophys. Res. Lett. 29*, 1535, doi:10.1029/2001GL013842

Chaston, C. C., et al. (2005), Energy deposition by Alfvén waves into the dayside auroral oval: Cluster and FAST observations, *J. Geophys. Res., 110*, A02211, doi:10.1029/2004JA010483.

Damiano, P.A. A.N. Wright, R.D. Sydora, and J.C. Samson (2007), Energy dissipation via electron energization in standing shear Alfvén waves. *Phys. Plasmas, 14*, 062904.

Damiano, P. A. and A. N. Wright (2008), Electron thermal effects in standing shear Alfvén waves, *J. Geophys. Res., 113*, A09219, doi:10.1029/2008JA013087.

Knudsen, D. (1996), Spatial modulation of electron energy and density by nonlinear stationary inertial Alfvén waves *J. Geophys. Res., 101*, 10,761-10,772.

Lotko, W., A.V. Streltsov, and C.W. Carlson (1998), Discrete auroral arc, electrostatic shock and suprathermal electrons powered by dispersive, anonamously resistive field

line resonance, *Geophys. Res. Lett., 25*, 4449-4452.

Lysak, R. L. and Y. Song (2003), Nonlocal kinetic theory of Alfvn waves on dipolar field lines, *J. Geophys. Res., 108*, 1327, doi:10.1029/2003JA009859.

Rankin, R., J.C. Samson, and V.T. Tikhonchuk (1999). Parallel electric fields in dispersive shear Alfvén waves in the dipolar magnetosphere. *Geophys. Res. Lett., 26*, 3601-3604.

Rankin, R., C.E.J. Watt, and J.C. Samson (2007), Self-consistent wave-particle interactions in dispersive scale long-period field line resonances, *Geophys., Res. Lett. 34*, L23103, doi:10.1029/2007GL031317.

Samson, J.C., R. Rankin, and V.T. Tikhonchuk (2003), Optical signatures of auroral arcs produced by field line resonances: comparison with satellite observations and modeling. *Ann. Geophys., 21*, 933-945.

Wright, A.N. W. Allan, M.S. Ruderman, and R.C. Elphic (2002), The dynamics of current carriers in standing Alfvén waves: Parallel electric fields in the auroral acceleration region. *J. Geophys. Res., 107*, 1120, doi:10.1029/2001JA900168.

Wright, A.N., W. Allan, and P.A. Damiano (2003), Alfvén wave dissipation via electron energization. *Geophys. Res. Lett., 30*, 1847, doi:10.1029/2003GL017605.

Xu, B.L., J.C. Samson, W.W. Liu, F. Creutzberg, and T.J. Hughes (1993). Observations of optical aurora modulated by resonant Alfvén waves. *J. Geophys. Res., 98*, 11,531-11,541.

Wygant, J., et al. (2000), Polar spacecraft based comparisons of intense electric fields and Poynting flux near and within the plasma sheet-tail lobe boundary to UVI images: An energy source for the aurora, *J. Geophys. Res., 105*, 18675-18692.
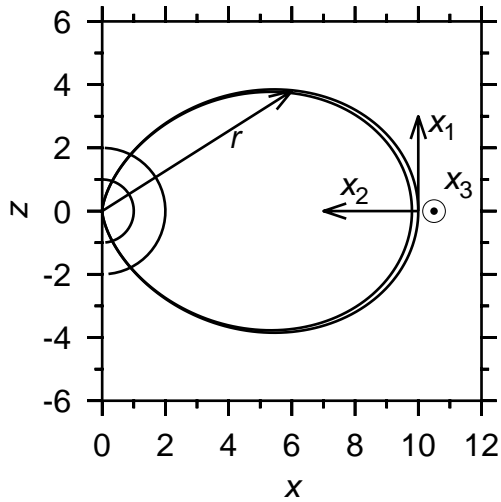
Figure 1. Simulation domain where x_3 is positive increasing out of the page. The circles of radius 1 and 2 R_E respectively denote the surface of the Earth and "ionospheric" boundary. The angle θ is subtended from the z axis. After Damiano et al., 2007.
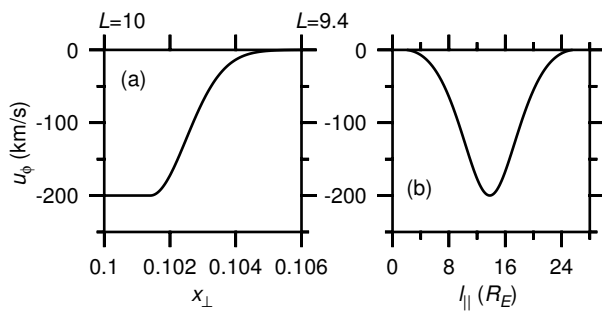

Figure 2. Azimuthal velocity perturbation as a function of: (a) x_2 at the equator and (b) length along the field line at $x_2 = 0.1$ (i.e. $L = 10$) where the length is measured from the southern ionospheric boundary.
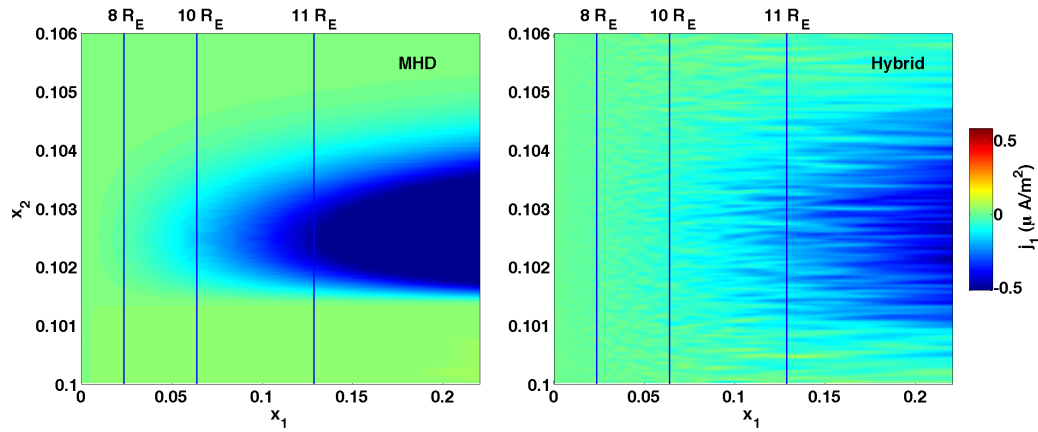
Figure 3. 2D plots of the northern hemisphere parallel electron current density for both the MHD (left) and hybrid (right) models at $t = 0.2\ T_A$. The left and right sides of each panel are the equator and northern ionospheric boundary respectively. The vertical lines in each panel indicate the noted distance from the equator.
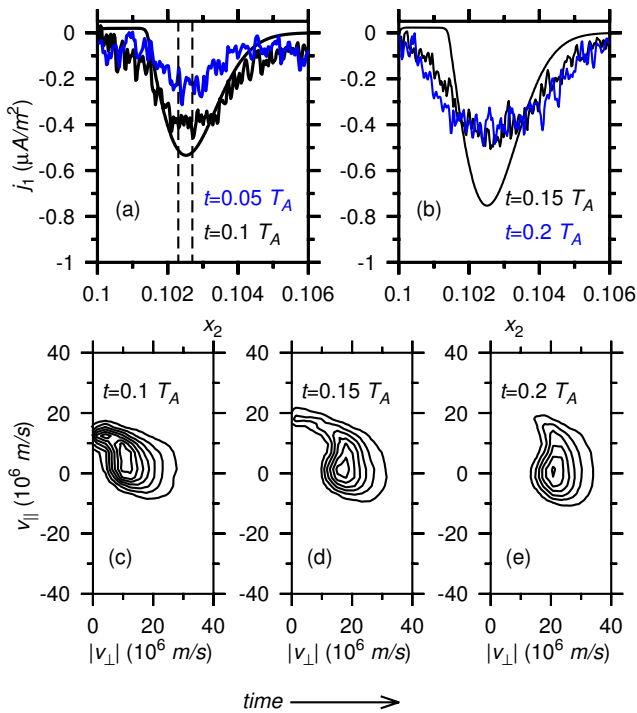
Figure 4. Top panels: j_1 at the northern ionospheric boundary at indicated times. Solid black line shows the MHD result. Bottom: Temporal distribution function evolution in region of max j_1 (vertical dashed lines in panel (a)). The distribution function is constructed using electrons with positions between these dashed lines and within the first two grid cells above the ionospheric boundary.
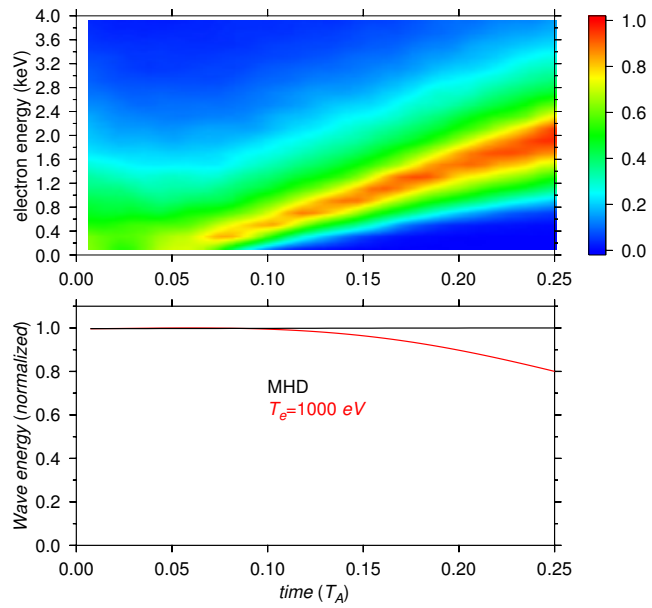
Figure 5. Top: Energy of the accelerated electron population in the region of the current maximum (vertical dashed lines in Figure 4a) as a function of time. Bottom: Sum of ion kinetic and magnetic energies.
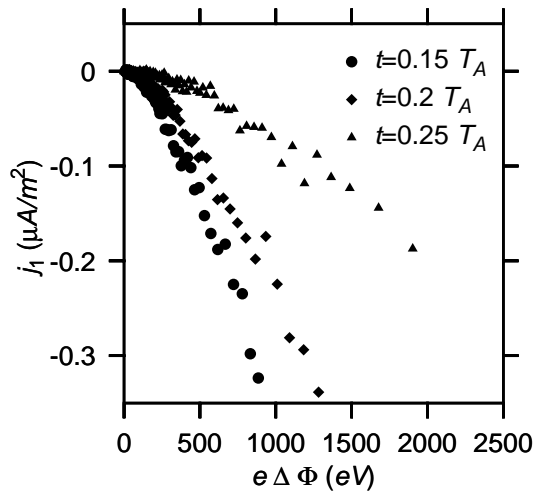

Figure 6. Parallel current density profile along $x_2 = 0.1025$ plotted against profile of potential along the same field line at indicated times. $\Delta\Phi$ was computed by integrating $E_{||}$ from the equator to individual grid points along the field line.

Information Services
Princeton Plasma Physics Laboratory
P.O. Box 451
Princeton, NJ 08543

Phone: 609-243-2245
Fax: 609-243-2751
e-mail: pppl_info@pppl.gov
Internet Address: http://www.pppl.gov